

Capacitive humidity sensing properties of carbon nanotubes grown on silicon nanoporous pillar array

JIANG WeiFen, XIAO ShunHua, ZHANG HuanYun, DONG YongFen & LI XinJian[†]

Department of Physics and Laboratory of Materials Physics, Zhengzhou University, Zhengzhou 450052, China

Multi-walled carbon nanotubes (CNTs) were grown on silicon nanoporous pillar array (Si-NPA) by thermal chemical vapor deposition method, and the structural and capacitive humidity sensing properties of CNT/Si-NPA were studied. It was found that with the relative humidity (RH) changing from 11% to 95%, a device response of ~480% was achieved at the frequency of 50000 Hz, and a linear device response curve could be obtained by adopting longitudinal logarithmic coordinate. The response/recovery times were measured to be ~20 s and ~10 s, respectively, which indicated a rather fast response/recovery rate. The adsorption-desorption dynamic cycle experiments demonstrated the high measurement reproducibility of CNT/Si-NPA sensors. These excellent performances were attributed to the unique surface structure, morphology and chemical inertness of CNT/Si-NPA.

capacitive humidity sensor, carbon nanotubes (CNTs), silicon nanoporous pillar array (Si-NPA), CNT/Si-NPA

Because the electric properties of carbon nanotubes (CNTs) are very sensitive to environments, CNT-based gas sensors, with both high sensitivity and high response speed, have been developed in detecting various toxic gases such as NO₂, H₂S and NH₃^[1-4]. Encouraged by the progress achieved in fabricating gas sensors, CNT-based humidity sensors, both resistive and capacitive types, have been probed by several groups in the past several years^[5,6]. Nevertheless, the sensing properties of CNT humidity sensors are presently far from device requirement. For example, the resistive sensors exhibited a rather low sensitivity and a very slow response/recovery speed^[5,6]. Although the sensitivity was greatly improved for capacitive sensors, the problem of slow response/recovery speed remains unsolved^[6]. In the papers published previously^[7-9], we reported the study on the capacitive humidity sensing properties of a silicon hierarchical structure, silicon nanoporous pillar array (Si-NPA), through which a very fast response/recovery speed was achieved. The excellent response/recovery behavior of Si-NPA-based sensors was attributed to the formation

Received December 3, 2006; accepted March 15, 2007

doi: 10.1007/s11431-007-0060-y

[†]Corresponding author (email: lixj@zzu.edu.cn)

Supported by the National Natural Science Foundation of China (Grant No. 10574112)

of a regular pillar array, which was believed to have brought an effective pathway for vapor transportation. In this paper, we will try to integrate the predominance of CNTs and Si-NPA to construct a novel humidity sensing composite, in an effort of obtaining good sensing performances. Here CNTs were grown on Si-NPA by thermal chemical vapor deposition (CVD) and the morphology and structure of CNT/Si-NPA were characterized by field emission scanning electron microscope (FE-SEM) and high resolution transmission electron microscope (HRTEM). The capacitive humidity sensing properties were measured and the sensing mechanism was analyzed based on the physical/chemical properties of CNTs and the structural characteristics of CNT/Si-NPA.

The preparation of Si-NPA substrate has been described in detail elsewhere^[7,8]. Si-NPA samples with an area of 20 mm×20 mm were dipped in a ferrocene/alcohol solution for 5 min, and then placed in a quartz tube furnace for growing CNTs by thermal CVD. The furnace was firstly heated up to 820°C under the protection of nitrogen gas, then maintained the temperature and changed the flowing gas to hydrogen. 20 min later, the flowing gas was changed to a mixture of hydrogen and nitrogen with 90 sccm (H₂:N₂=3:6, volume ratio). In the process, a feed solution of xylene was carried into the furnace by flowing gas at a rate of 0.2 ml/min. The carbon atoms needed for CNT growing was provided by the thermal decomposition of xylene. The growing process lasted 5 min. Then the flowing gas was changed to nitrogen again and the inner temperature of the furnace was naturally cooled down to room temperature.

Planar, interdigital aluminum electrodes were formed on CNT/Si-NPA by thermal evaporation technique. The capacitive sensing properties were studied through measuring the device capacitance under different humidity environments, which were achieved by encapsulating saturated aqueous solutions of LiCl, MgCl₂, Mg(NO₃)₂, NaCl, KCl and KNO₃ in glass vessels at room temperature. The produced relative humidity (RH) were 11.3%, 33.1%, 54.4%, 75.5%, 85.1% and 94.6%, respectively. The capacitance responses of CNT/Si-NPA to humidity were measured with a TH2818 Automatic Component Analyzer/Precision LCR multi-frequency meter. The frequency scale of the equipment was 20—300 kHz.

Figure 1(a) presents the surface morphology of Si-NPA obtained by FE-SEM, where a regular array composed of large quantities, well-separated, quasi-identical silicon pillars could be observed. The height of the pillars was ~3 μm and the distance between every two neighboring pillars was ~4.0 μm. The valleys around the pillars were well connected and formed an effective pathway for vapor transportation. The surface morphology of CNT/Si-NPA is shown in Figure 1(b), where numerous entangled CNTs could be observed. From the amplified FE-SEM image given in Figure 1(c), it could be seen that CNT assemblages have been formed at the top of silicon pillars. Figure 1(d) is the HRTEM image of an individual CNT, from which it could be judged that as-grown CNTs are multi-walled CNTs. The diameter of this CNT is ~24 nm and the tube wall contains 13 graphitic layers.

It is known that for capacitive humidity sensors, the variation of capacitance highly depends upon the applied signal frequency. To find the frequency which is most suitable for CNT/Si-NPA sensors, a series of capacitance-RH curves were measured at 100, 2000, 10000, 50000 and 200000 Hz, and the results were depicted in Figure 2(a). Clearly, the lower the applied frequency, the larger the capacitance difference when RH between 11% and 95%. For example, when RH was changed from 11% to 95%, the corresponding capacitance increments was ~2600% at 100 Hz and ~220% at 200000 Hz, respectively. Compared with resistive humidity sensors whose resistance increments

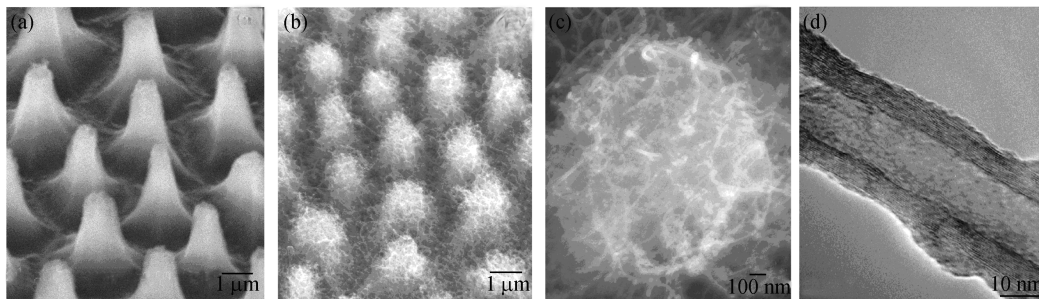


Figure 1 FE-SEM images of Si-NPA tilted with an angle of 45° (a), CNT/Si-NPA tilted with an angle of 30° (b), an individual CNT nest (c), and TEM image of an individual CNT (d).

are usually below 20%, the maximum variation in the measuring RH scale is high enough even at 200000 Hz. But it should be noted that the capacitance-RH curve is far from linearity. This is a common problem met for capacitive humidity sensors and constructs a big barrier to be overcome^[10–12]. According to the analysis given by other groups^[13–15], the non-linear capacitance-RH response should be attributed to the long relaxation time of dipole moments of adsorbed water molecules and the vapor condensation occurred at high humidity environment. This means that the non-linear capacitance response to humidity could not be cancelled through device designing or material choosing. Therefore, data transformation might be a possible way to realize a linear device response. To achieve this goal, we firstly define the device response (C_{DEV}) as

$$C_{DEV} = \frac{C_{RH} - C_{11}}{C_{11}} \times 100\%,$$

where C_{11} and C_{RH} represent the capacitance at RH = 11% and at a certain measuring humidity levels, respectively. The obtained C_{DEV} -RH curves with different frequencies are presented in Figure 2(b). Through the technical transformation, the capacitance variation with RH was enlarged, but the linearity of the C_{DEV} -RH curve was still poor. Figure 2(c) presents the C_{DEV} -RH curves re-plotted by replacing the longitudinal coordinates with the logarithm of C_{DEV} . Clearly, the linearity of all these response curves was greatly improved, in which the curve corresponding to 50000 Hz was of the highest linearity. Therefore, 50000 Hz was the most suitable signal frequency for a CNT/Si-NPA capacitive humidity sensor and in the following measurements, the signal frequency was always chosen as 50000 Hz. Figure 2(d) presents the C_{DEV} -RH curve of CNT/Si-NPA measured at 50000 Hz and that of Si-NPA substrate as a comparison, whose maximum device responses are ~480% and ~160%, respectively. Judged from value of device response, CNT/Si-NPA possesses obvious predominance over Si-NPA.

Response/recovery times are also the most important parameters for all humidity sensors. Figure 3(a) shows the response/recovery time curves of a CNT/Si-NPA sensor in an RH-increasing and an RH-decreasing process with RH ranging from 11% to 85%. By defining the time taken to achieve 90% of its total capacitance variation as device response/recovery times, the response time and recovery time of CNT/Si-NPA sensor were measured to be ~20 s and ~10 s, respectively. Compared with the corresponding values of Si-NPA (~27 s and ~2 s)^[9], the response time was shortened by ~7 s but the recovery time was prolonged by ~8 s. This makes more balanced response/recovery times and would be more helpful for a practical sensor. The mechanism might be as follows. As has been proved previously^[8], Si-NPA possessed a nanoporous surface structure similar to that of

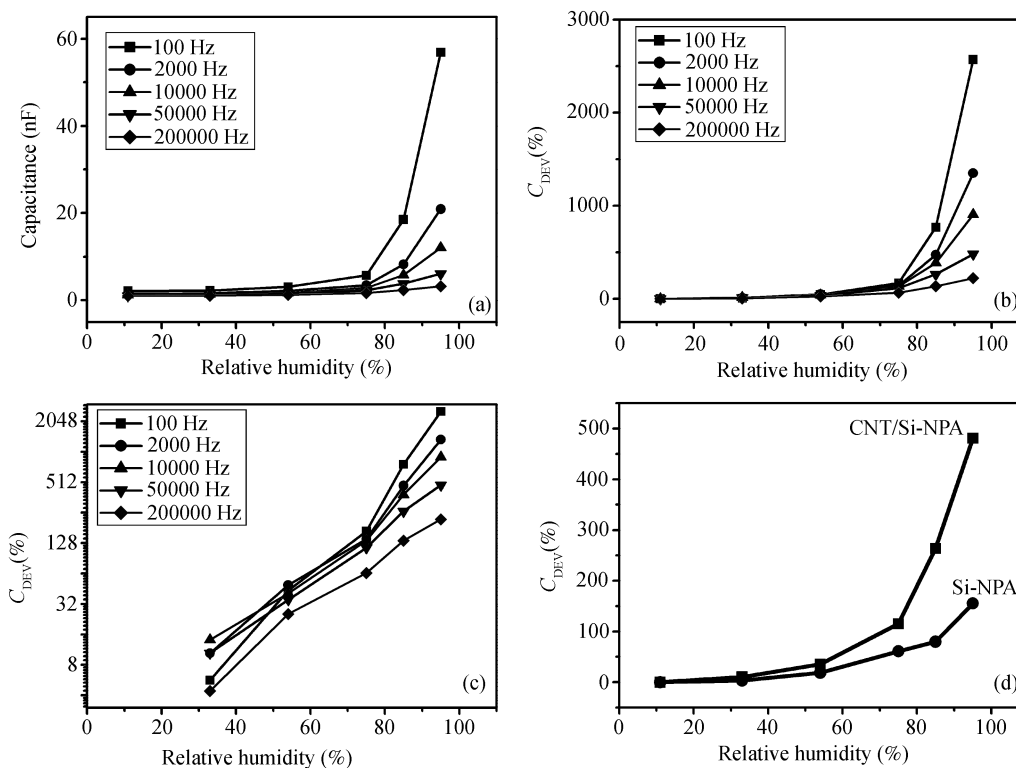


Figure 2 Experimental capacitance-RH curves measured with frequencies of 100, 2000, 10000, 50000 and 200000 Hz (a), the transformed C_{DEV} -RH curves (b), the re-plotted C_{DEV} -RH curves by longitudinal logarithmic coordinate (c) and C_{DEV} -RH curves of CNT/Si-NPA and Si-NPA measured at 50000 Hz (d).

traditional porous silicon (PS). The surface of PS has been proved to be hydrophobic^[16–18], which would lead to the surface being difficult for vapor adsorption but easy for vapor desorption. Therefore, the response time of Si-NPA was a little longer than the recovery time. Although a perfect CNT surface was also proved to be hydrophobic^[19,20], it was demonstrated that any oxidation or contamination of CNTs would lead to considerable affinity for vapor molecule^[6,21]. Therefore in the case of CNT/Si-NPA, the growing process and the precursors decided that as-grown CNTs were impossible to be defect-free. Therefore the response time of CNT/Si-NPA was shortened and the recovery time was prolonged compared with those of Si-NPA. Compared with the popularly studied porous SiC capacitive humidity sensor^[22], whose best response/recovery times were ~ 120 s and ~ 90 s, respectively, CNT/Si-NPA was no doubt to be more practical. Considering the morphological properties of CNT/Si-NPA, we tend to think that the faster response rate might be attributed to the regular hierarchical structure of Si-NPA substrate (Figure 1(a)). It is easy to find that all the trenches surrounding silicon pillars were well connected and composed of a channel network. It is the well established channel network that might have constructed an effective pathway for water vapor transportation, and finally led to the increment of the adsorption and desorption rate of water molecules on or from the surface of CNT/Si-NPA.

The measurement reproducibility of CNT/Si-NPA sensors were tested through carrying out the adsorption-desorption dynamic cycles, in which the RH levels of the testing environment were interchanged between 11% and 85% repeatedly. The experimental device response-time curve of

four dynamic cycles is depicted in Figure 4, which exhibits rather high identity at different RH dynamic cycles and indicates the capacitive humidity sensing properties of CNT/Si-NPA is stable.

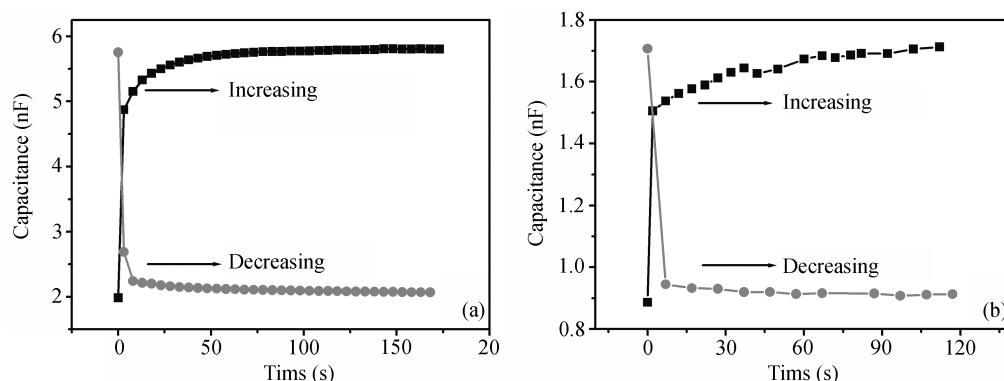


Figure 3 The experimental data on measuring response/recovery times of CNT/Si-NPA (a) and Si-NPA (b). The ascending and descending curves correspond to response process (RH: 11%–85%) and the recovery process (RH: 85%–11%), respectively.

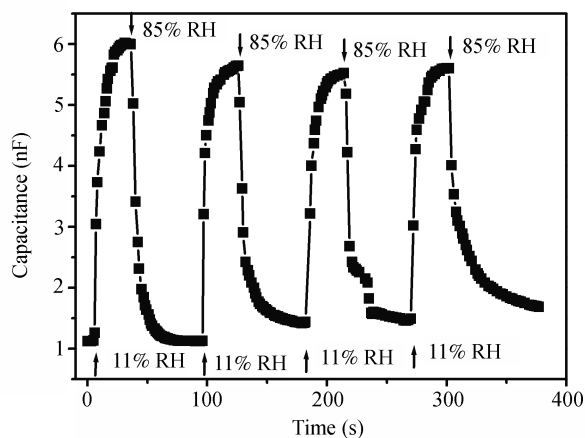


Figure 4 Demonstration of the measurement reproducibility of CNT/Si-NPA carried out by adsorption-desorption dynamic cycles, in which the RH levels of the testing environment were interchanged between 11% and 85% repeatedly.

In conclusion, a novel composite CNT/Si-NPA was prepared and based on it a capacitive humidity sensor was fabricated. The capacitive humidity sensing properties of CNT/Si-NPA were measured at room temperature. Our results show that as-prepared CNT/Si-NPA could exhibit high sensitivity, short response/recovery times and good measurement reproducibility. These excellent performances of CNT/Si-NPA are attributed to the unique surface structure, morphology and chemical inertness of CNT/Si-NPA.

- 1 Valentini L, Armentano I, Kenny J M, et al. Sensors for sub-ppm NO₂ gas detection based on carbon nanotube thin films. *Appl Phys Lett*, 2003, 82: 961–963
- 2 Lawrence N S, Deo R P, Wang J. Electrochemical determination of hydrogen sulfide at carbon nanotube modified electrodes. *Anal Chim Acta*, 2004, 517: 131–137
- 3 Jang Y -T, Moon S -I, Ahn J -H, et al. A simple approach in fabricating chemical sensor using laterally grown multi-walled carbon nanotubes. *Sens Actuat B*, 2004, 99: 118–122
- 4 Kong J, Franklin N R, Zhou C, et al. Nanotube molecular wires as chemical sensors. *Science*, 2000, 287: 622–625
- 5 Cantalini C, Valentini L, Armentano I, et al. Sensitivity to NO₂ and cross-sensitivity analysis to NH₃, ethanol and humidity

- of carbon nanotube thin film prepared by PECVD. *Sens Actuat B*, 2003, 95: 195–202
- 6 Varghese O K, Kichambre P D, Gong D, et al. Gas sensing characteristics of multi-wall carbon nanotubes. *Sens Actuat B*, 2001, 81: 32–41
 - 7 Li X J, Hu X, Jia Y, et al. Tunable superstructures in hydrothermally etched iron-passivated porous silicon. *Appl Phys Lett*, 1999, 75: 2906–2908
 - 8 Xu H J, Fu X N, Sun X R, et al. Investigations on the structural and optical properties of silicon nanoporous pillar array. *Acta Phys Sin*, 2005, 54: 2352–2357
 - 9 Xu Y Y, Li X J, He J T, et al. Capacitive humidity sensing properties of hydrothermally-etched silicon nano-porous pillar array. *Sens Actuat B*, 2005, 105: 219–222
 - 10 Das J, Hossain S M, Chakraborty S, et al. Role of parasitics in humidity sensing by porous silicon. *Sens Actuat A*, 2001, 94: 44–52
 - 11 Kumar B P, Kumar H H, Kharat D K. Effect of porosity on dielectric properties and microstructure of porous PZT ceramics. *Mater Sci Eng B*, 2006, 127: 130–133
 - 12 Viviani M, Buscaglia M T, Buscaglia V, et al. Barium perovskites as humidity sensing materials. *J Europ Ceram Soc*, 2001, 21: 1981–1984
 - 13 Kim S J, Park J Y, Lee S H, et al. Humidity sensors using porous silicon layer with mesa structure. *J Phys D*, 2000, 33: 1781–1784
 - 14 Zahab A, Spina L, Poncharal P, et al. Water-vapor effect on the electrical conductivity of a single-walled carbon nanotube mat. *Phys Rev B*, 2000, 62: 10000–10003
 - 15 Na P S, Kim H, So H -M, et al. Investigation of the humidity effect on the electrical properties of single-walled carbon nanotube transistors. *Appl Phys Lett*, 2005, 87: 093101
 - 16 Halimaoui A. Influence of wettability on anodic bias induced electroluminescence in porous silicon. *Appl Phys Lett*, 1993, 63 (9):1264–1266
 - 17 Salonen J, Björkqvist M, Laine E, et al. Stabilization of porous silicon surface by thermal decomposition of acetylene. *Appl Surf Sci*, 2004, 225: 389–394
 - 18 Jin W J, Shen G L, Yu R Q. Organic solvent induced quenching of porous silicon photoluminescence. *Spectrochim Acta Part A*, 1998, 54: 1407–1414
 - 19 Valentini L, Armentano I, Kenny J M. Electrically switchable carbon nanotubes hydrophobic surfaces. *Diam Relat Mater*, 2005, 14: 121–124
 - 20 Musso S, Porro S, Rovere M, et al. Physical and mechanical properties of thick self-standing layers of multiwall carbon nanotubes. *Diam Relat Mater*, 2007, 16: 1174–1178
 - 21 Gogotsi Y, Naguib N, Libera J A. In situ chemical experiments in carbon nanotubes. *Chem Phys Lett*, 2002, 365: 354–360
 - 22 Connolly E J, O'Halloran G M, Pham H T M, et al. Comparison of porous silicon, porous polysilicon and porous silicon carbide as materials for humidity sensing applications. *Sens Actuat A*, 2002, 99: 25–30